Magnetic ordering and dense Kondo behavior in $EuFe_2P_2$

Chunmu Feng
Department of Physics, Zhejiang University, Hangzhou 310027, China
and Test and Analysis Center, Zhejiang University, Hangzhou 310027, China

Zhi Ren, Shenggao Xu, Shuai Jiang, Zhu'an Xu, and Guanghan Cao*
Department of Physics, Zhejiang University, Hangzhou 310027, China and State Key Lab of Silicon Materials, Zhejiang University, Hangzhou 310027, China

I. Nowik and I. Felner
Racah Institute of Physics, The Hebrew University, Jerusalem 91904, Israel

Kazuyuki Matsubayashi and Yoshiya Uwatoko
Institute for Solid State Physics, The University of Tokyo, Kashiwanoha, Kashiwa, Chiba 277-8581, Japan
(Received 16 July 2010; published 15 September 2010)

Ternary iron phosphide $EuFe_2P_2$ with $ThCr_2Si_2$-type structure has been systematically studied by the measurements of crystal structure, magnetization, Mössbauer effect, transport properties, and specific heat. The structural refinement result confirms no direct P-P covalent bonding. The Mössbauer spectra indicate no magnetic moment for the Fe atoms and that the Eu ions are divalent in the whole temperatures. The Eu^{2+} spins order ferromagnetically at $T_C=29$ K, followed by a possible helimagnetic ordering below $T_{HM}=26$ K, where the Eu^{2+} moments tilt a little from the c axis. External magnetic field increases the T_C gradually but suppresses the T_{HM} rapidly. (Magneto)resistivity data indicate characteristic dense Kondo behavior above the Curie temperature. The result is discussed in terms of the interplay between intersite Ruderman-Kittel-Kasuya-Yosida and intrasite Kondo interactions.

DOI: 10.1103/PhysRevB.82.094426 PACS number(s): 75.50.Cc, 75.30.Cr, 75.30.Mb, 76.80.+y

I. INTRODUCTION

The interplay between $4f$ and conduction electrons in intermetallic compounds has led to a wide variety of novel ground states,[1,2] attracting sustained interest in condensed matter physics community. In the pnictide family, EuT_2Pn_2 (T=transition metals; Pn=As or P) offers us a rare opportunity to access such an interplay. The ternary compound crystallizes in $ThCr_2Si_2$-type structure, consisting of Eu sublattice with $4f$ electrons and T sublattice with $3d$ electrons. Europium is known as a special rare-earth element due to the two stable valence configurations: Eu^{2+} and Eu^{3+}, showing a large moment ($J=S=7/2$) and zero moment ($J=0$), respectively. In most cases, europium shows the lower valence with high magnetic moment, which renders magnetically ordered ground states. However, mixed-valence state for Eu was evidenced by Mössbauer investigations in a "collapsed" phase $EuNi_2P_2$.[3] By applying pressures, a structural transition toward the collapsed phase was observed in $EuCo_2P_2$ and $EuFe_2P_2$, accompanying with a partial valence transition.[4,5] In earlier studies, valence fluctuations of Eu were also demonstrated in $EuCu_2Si_2$ system.[6,7]

The europium iron pnictide $EuFe_2Pn_2$, first synthesized more than 30 years ago,[8] exhibits totally different physical properties for Pn=As and P. $EuFe_2As_2$ undergoes a spin-density-wave transition in the Fe sublattice at 200 K, followed by an AFM ordering of Eu^{2+} moments at 20 K.[9–11] By contrast, as reported in Ref. 3, the Fe atoms do not carry local moments while the Eu^{2+} spins order ferromagnetically (FM) at 27 K in $EuFe_2P_2$. Surprisingly, by doping P into $EuFe_2As_2$, both superconductivity coming from Fe $3d$ electrons and ferromagnetism due to Eu $4f$ moments were observed in $EuFe_2(As_{0.7}P_{0.3})_2$.[12]

While $EuFe_2As_2$ has been extensively studied recently,[10,11,13–19] few works[3–5] have been devoted to $EuFe_2P_2$. To the best of our knowledge, the transport and thermodynamic properties of $EuFe_2P_2$ have not been reported so far. Moreover, the contrasting behaviors between an iron arsenide and its sister phosphide are explicitly demonstrated in CeFePnO system: CeFeAsO serves as a parent compound for high-temperature superconductors[20] but CeFePO has been recognized as a heavy Fermion metal with ferromagnetic correlation.[21] Therefore, what $EuFe_2P_2$ behaves is an important issue to be investigated. In this paper, we performed a systematic study on $EuFe_2P_2$ by the measurements of crystal structure, transport properties, specific heat, as well as magnetic properties and Mössbauer spectra. The Eu valence state is confirmed to be 2+ in the whole temperatures and the Eu^{2+} moments order in a complex manner rather than the simple reported ferromagnetism at low temperatures. Strikingly, $EuFe_2P_2$ shows a dense Kondo behavior. Our result demonstrates that, as an Eu-containing compound, $EuFe_2P_2$ sets a rare example displaying the interplay between Kondo and Ruderman-Kittel-Kasuya-Yosida (RKKY) interactions.

II. EXPERIMENTAL DETAILS

Polycrystalline samples of $EuFe_2P_2$ were synthesized by solid-state reaction between EuP and Fe_2P, as reported previously.[12] EuP was presynthesized by heating europium

grains and phosphorus powders very slowly to 1173 K, then holding for 36 h. Fe_2P was presynthesized by reacting iron and phosphorus powders at 973 K for 24 h from stoichiometric amounts of the elements. All the starting materials have the purity better than 99.9%. Powders of EuP and Fe_2P were weighed according to the stoichiometric ratio, thoroughly ground and pressed into pellets in an argon-filled glove box. The pellets were then sealed in an evacuated quartz tube and sintered at 1273 K for 36 h then cooled slowly to room temperature.

Powder x-ray diffraction (XRD) was carried out using a D/Max-rA diffractometer with Cu $K\alpha$ radiation and a graphite monochromator. The structural refinement was performed using the program RIETAN 2000.[22] The electrical resistivity was measured using a standard four-probe method. Thermoelectric power measurements were carried out by a steady-state technique with a temperature gradient ~1 K/cm. Magnetoresistance (MR) and specific-heat measurements were performed on a Quantum Design physical property measurement system (PPMS-9). The dc magnetization was measured on a Quantum Design magnetic property measurement system (MPMS-5).

Mössbauer studies were performed using a conventional constant acceleration drive. The sources were 50 mCi ^{57}Co:Rh for ^{57}Fe spectra and 200 mCi $^{151}Sm_2O_3$ source for the ^{151}Eu spectra. The absorbers were measured in a Janis model SHI-850-5 closed cycle refrigerator. The spectra were analyzed in terms of least-square fit procedures to theoretical expected spectra, including full diagonalization of the hyperfine interaction spin Hamiltonian. The analysis of the ^{151}Eu spectra considered also the exact shape of the source emission line, as shown in Ref. 23. The velocity calibration was performed with an α-iron foil at room temperature. The reported isomer-shift (IS) values for iron are relative to the Fe foil, for europium relative to the oxide source at room temperature.

III. RESULTS AND DISCUSSION

A. Crystal structure

Figure 1 shows the powder XRD pattern for the as-prepared $EuFe_2P_2$ sample. No obvious secondary phase can be detected. By employing $ThCr_2Si_2$-type structure with the space group of $I4/mmm$, the crystal structure were successfully refined (the reliable factor R_{wp}=0.098; the goodness of fit is 1.61). The fitted lattice parameters are a =3.8178(1) Å and c=11.2372(3) Å, in agreement with the literature values [a=3.818(1) Å and c=11.224(4) Å].[8] Compared with the counterpart of arsenide $EuFe_2As_2$,[11] the a and c axes decrease by 2.3% and 7.3%, respectively. The larger decrease in c axis suggests stronger interlayer coupling.

Detailed structural comparison between $EuFe_2P_2$ and $EuFe_2As_2$ can be seen in Table I. The position of phosphorus is closer to the iron planes, which leads to 13.7% decrease in the thickness of Fe_2Pn_2 layers. On the other hand, the spacing of Fe_2Pn_2 layers, namely, the *Pn*-*Pn* distance, only decreases by 2.1%. One note that the P-P distance (3.263 Å) in $EuFe_2P_2$ is much larger than the threshold value of ~2.3 Å

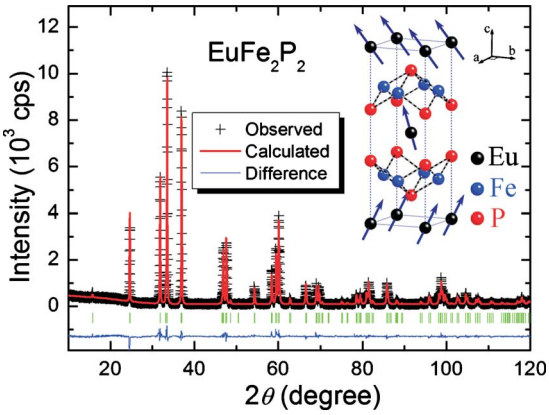

FIG. 1. (Color online) Rietveld refinement profile of powder x-ray diffraction at room temperature for $EuFe_2P_2$. The inset shows the crystal structure. A possible magnetic structure is also illustrated based on the magnetization and Mössbauer results.

(Ref. 24) for the P-P bonding along the c axis. Therefore, unlike the collapsed phase $EuNi_2P_2$,[3] there is no covalent P-P bonding in $EuFe_2P_2$ at ambient condition. This result is consistent with the previous report.[4] In the concept of bond valence sum,[25] the formal valence of Eu is calculated to be 1.89 using the Eu-P bond length data and the related parameters.[26]

B. Magnetization

Although the XRD experiment shows no obvious secondary phase, the magnetic measurement indicates a steplike decrease in susceptibility from 200 to 300 K (not shown here). Similar phenomena was observed previously in the $EuFe_2(As_{0.7}P_{0.3})_2$ sample,[12] which is due to the presence of trace amount of ferromagnetic impurity Fe_2P with a Curie point at 306 K.[27] The molar fraction of Fe_2P was estimated to be below 1% from the $M(H)$ curves at 100 K. Figure 2(a) shows the temperature dependence of magnetic susceptibility (χ) below 120 K for the $EuFe_2P_2$ sample. The data of 35 K$\leq T\leq$120 K follow the modified Curie-Weiss law,

TABLE I. Comparison of room-temperature crystal structures for $EuFe_2As_2$ (Ref. 11) and $EuFe_2P_2$ (this work). The atomic coordinates of Eu, Fe and *Pn* are (0, 0, 0), (0.5, 0, 0.25), and (0, 0, z), respectively.

Compounds	$EuFe_2As_2$	$EuFe_2P_2$
Space group	$I4/mmm$	$I4/mmm$
a (Å)	3.9062(3)	3.8178(1)
c (Å)	12.1247(2)	11.2372(3)
V (Å^3)	185.01(1)	163.79(1)
z of *Pn*	0.3625(1)	0.3548(2)
Fe_2Pn_2-layer thickness (Å)	2.728(2)	2.355(2)
Pn-*Pn* distance (Å)	3.333(2)	3.263(2)
Eu-*Pn* bond length (Å)	3.226(2)	3.154(2)
Pn-Fe-*Pn* angle (deg)	110.1(1)	116.7(1)
Bond valence sum for Eu	1.93	1.89

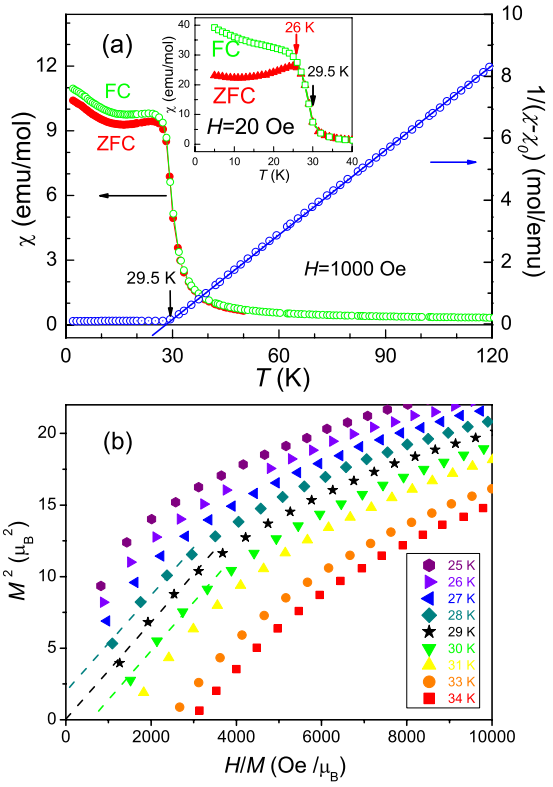

FIG. 2. (Color online) (a) Temperature dependence of magnetic susceptibility measured under $H=1$ kOe for $EuFe_2P_2$. The low-field susceptibility data ($H=20$ Oe) is shown in the inset. (b) An Arrot plot for $EuFe_2P_2$.

$$\chi = \chi_0 + \frac{C}{T-\theta}, \tag{1}$$

where χ_0 denotes the temperature-independent term, C the Curie-Weiss constant, and θ the paramagnetic Curie temperature. The fitted value of χ_0 is as high as 0.22 emu/mol, which is mainly ascribed to the ferromagnetic Fe_2P impurity. The fitting also yields the effective magnetic moments $P_{eff}=8.3\ \mu_B$ per formula unit and $\theta=29$ K. The P_{eff} value is consistent with the theoretical value of 7.94 μ_B for a free Eu^{2+} ion (The slightly larger value is also due to the influence of the tiny Fe_2P impurity). A ferromagnetic transition is manifested by the rapid increase in χ below 30 K, as well as the divergence of zero-field-cooling (ZFC) and fied-cooling (FC) data. This result is basically consistent with the previous report claiming FM transition at 27 K by Mössbauer and magnetic-susceptibility investigations.[3] However, the Curie point (T_C) has 2 K difference. In fact, precise determination of the T_C by a single $M(T)$ curve is difficult because of the large moments of Eu^{2+}. We thus measured series of $M(H)$ curves nearby T_C. The data are shown in the plot of M^2 vs H/M (so-called Arrot plot), which clearly indicates that the Curie temperature is 29 K.

Below the T_C, we note a kink at 26 K in the $\chi(T)$ data [shown in the inset of Fig. 2(a)], which is quite different from those of the conventional ferromagnet. The temperature dependence of magnetization under various fields is displayed in Fig. 3. For high magnetic fields, say $\mu_0 H=1$ T, the magnetization approximately saturates to the theoretical value of $gS=7.0\ \mu_B$/f.u. at 2 K. In the case of low fields, however, there is another magnetic transition below T_C, characterized by the temperature-independent magnetization. This phenomenon is very much similar to that in $Eu(Fe_{0.89}Co_{0.11})_2As_2$,[28] where a helimagnetism (HM) was proposed. In the HM state, as illustrated in the inset of Fig. 1, the Eu^{2+} spins align ferromagnetically within the Eu atomic planes but the interlayer spin directions differ in a fixed angle. Note that the ^{151}Eu Mössbauer study below indicates that the spin direction tilts about 20° from the c axis, which gives rise to the observed macroscopic ferromagnetism. External field suppresses the T_{HM} rapidly but increases the T_C gradually. The stabilization of FM state by the external field was explained in our previous paper.[28]

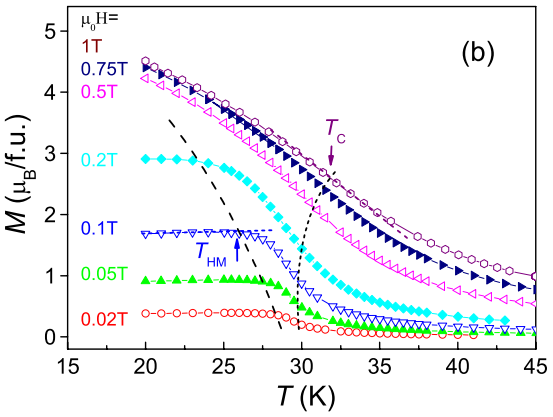

FIG. 3. (Color online) Temperature dependence of magnetization under various magnetic fields for $EuFe_2P_2$. T_C and T_{HM} denote the ferromagnetic and helimagnetic transition temperatures, respectively.

The dominant ferromagnetism in $EuFe_2P_2$ is further demonstrated by the field-dependent magnetization, shown in Fig. 4. The magnetization increases steeply with initially increasing H and tends to saturate for $H \geq 10^4$ Oe. The saturated magnetic moment is ~6.7 μ_B/f.u., close to the expected value of 7.0 μ_B/f.u. In addition, a small hysteresis loop is presented on closer examination. All these features

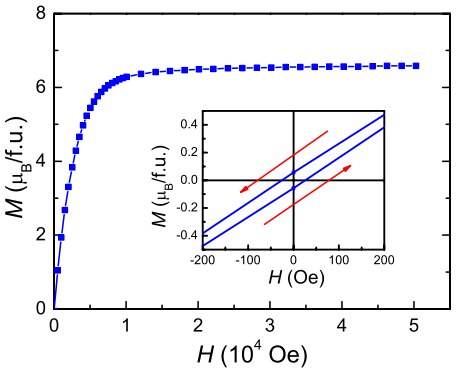

FIG. 4. (Color online) Field dependence of magnetization at 2 K for $EuFe_2P_2$. The inset shows tiny magnetic hysteresis with the coercive field of only 30 Oe.

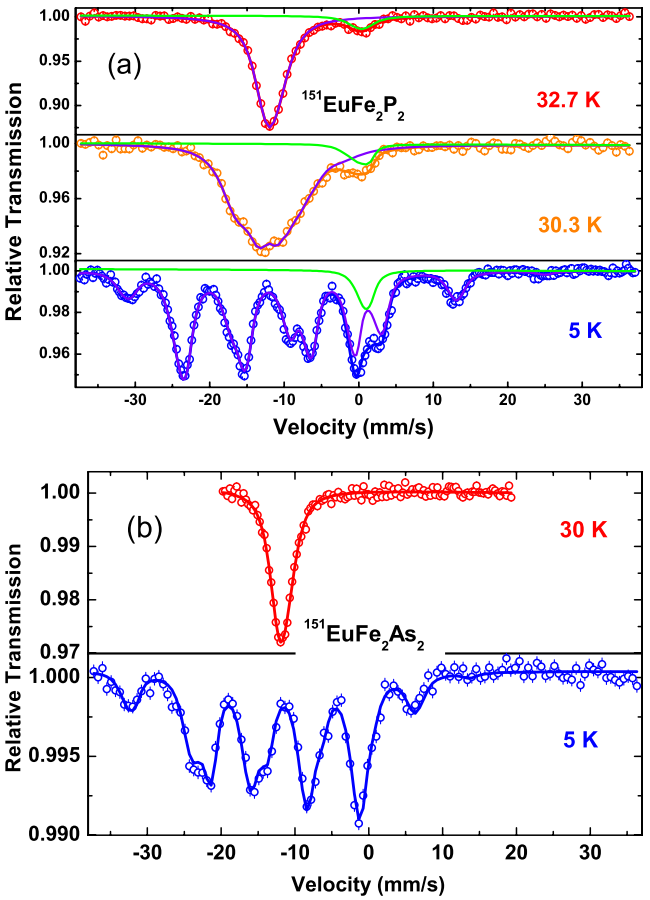

FIG. 5. (Color online) (a) ^{151}Eu Mössbauer spectra of $EuFe_2P_2$, below (5 K), around (30.3 K), and above (32.7 K) the ferromagnetic ordering temperature of the Eu sublattice. The observed impurity site is probably due to minor Eu_2O_3 on the surface of the grains. The hyperfine field is basically along the c axis. (b) ^{151}Eu Mössbauer spectra of $EuFe_2As_2$, below (5 K) and above (30.0 K) the antiferromagnetic ordering temperature of the Eu sublattice. The hyperfine field (26.2 T) is perpendicular to the c axis.

are consistent with basically ferromagnetic alignment of Eu^{2+} moments.

C. Mössbauer spectra

Mössbauer spectroscopy studies of ^{151}Eu and ^{57}Fe in the system $EuFe_2P_2$ at temperatures 5–297 K have been performed. A previous study of this compound has been reported in Ref. 3.

^{151}Eu spectra [Fig. 5(a)] display pure quadrupole interactions down to the magnetic ordering temperature of the Eu sublattice. The values of the measured IS are −11.0(1) mm/s at 297 K, −11.4(1) mm/s at 40 K, and −11.3(1) mm/s at 5 K, proving that the Eu ions are divalent at all temperatures. The quadrupole interaction values $(\frac{1}{4}e^2qQ_0)$ are −2.32(2) mm/s at 297 K and −2.55(2) mm/s at 40 K. At 5 K, the quadrupole shift is −2.95(2) mm/s and the magnetic hyperfine field (H_{eff}) is 30.1(1) T. The quadrupole shift value at 5 K, when analyzed in the approximation that the magnetic interactions are much larger than the quadrupole interaction, indicates that H_{eff} points along the crystalline c axis, the major axis of the axial electric field gradient producing the quadrupole interaction. However, analyzing the spectrum with a full diagonalization of the hyperfine spin Hamiltonian gives a better fit when the hyperfine field tilts away from the c axis by 20(5)°. This is in contrast to $EuFe_2As_2$ [Fig. 5(b)], where the Eu moments order antiferromagnetically (of A type) and the hyperfine field is perpendicular to the c axis. The same phenomenon is also observed in $Eu(Fe_{0.9}Ni_{0.1})_2As_2$,[29] where the Eu moment is ferromagnetically ordered.[30] The observed H_{eff} in $EuFe_2P_2$ is higher than that (H_{eff}=26.2 T) in $EuFe_2As_2$.

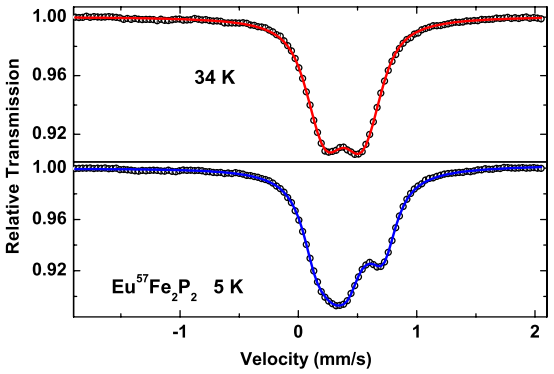

FIG. 6. (Color online) ^{57}Fe Mössbauer spectra of $EuFe_2P_2$, below (5 K) and above (34 K) the ferromagnetic ordering temperature of the Eu sublattice. The transferred magnetic hyperfine field at 5 K is along the c axis.

The ^{57}Fe Mössbauer spectra display a pure quadrupole splitting down to T_C. The measured IS are 0.28 mm/s at room temperature, 0.38 mm/s at 34 K, and 0.39 mm/s at 5 K. The quadrupole interaction $(\frac{1}{4}e^2qQ_0)$ values are 0.16(1) mm/s at 297 K, 0.15(1) mm/s at 30 K, and below T_C, at 5 K, 0.17(1) mm/s. A small foreign phase (probably Fe_2P) of less than 5% is also present. In Fig. 6 one can observe the change in the spectrum between 34 and 5 K. No Fe magnetic moment is evidenced. At 5 K the spectrum displays a small magnetic hyperfine field [H_{eff}=0.97(2) T], acting on the iron nucleus. This small field is a transferred field from the ferromagnetically ordered Eu sublattice, as previously observed.[3] It was also observed in ferromagnetic $Eu(Fe_{0.9}Ni_{0.1})_2As_2$.[29] This transferred field seems to point along the c axis, however analyzing the spectrum with a full diagonalization of the hyperfine spin Hamiltonian produces a better fit when the H_{eff} tilts from the c axis by 15(5)°. Thus our measurements show, that the transferred field on the iron site, points in the same direction as that of the Eu magnetic moment.

D. Transport properties

1. Resistivity and magnetoresistivity

For intermetallic compounds, dense polycrystalline samples largely exhibit intrinsic transport properties as single crystals do because of well electrical contact between crystalline grains. Thus our sample, which had metal luster by polishing, may reflect the intrinsic transport properties. Fig-

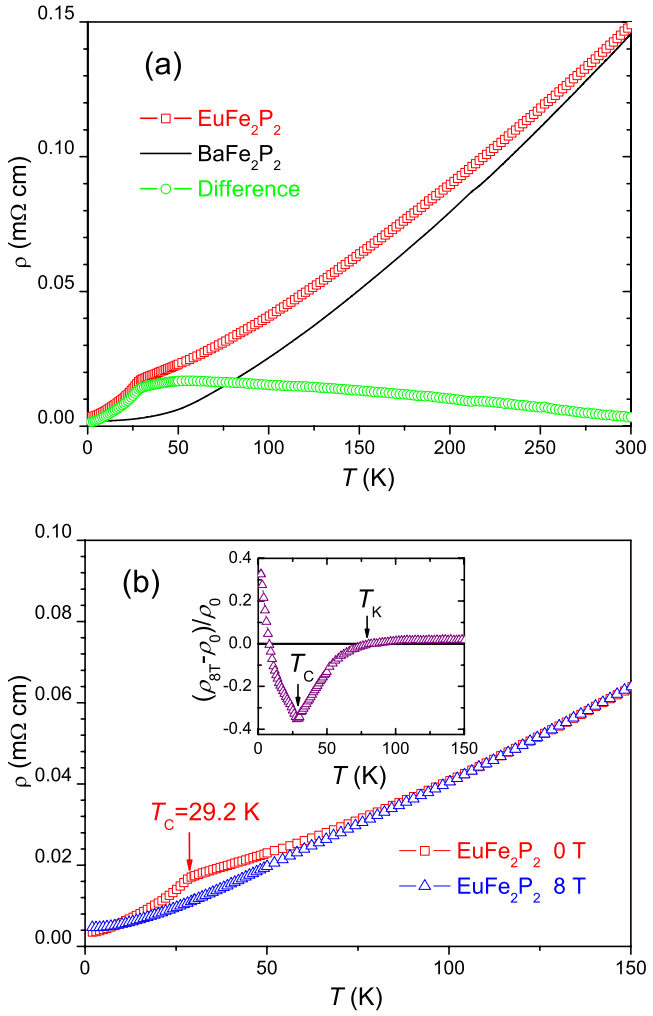

FIG. 7. (Color online) (a) Temperature dependence of resistivity for $EuFe_2P_2$. The $\rho(T)$ data of $BaFe_2P_2$ are also plotted for comparison. The circle symbols denote the difference (by a subtraction), which basically represents the resistivity contribution from magnetic scattering. (b) Anomalous temperature dependence of magnetoresistance in $EuFe_2P_2$.

ure 7(a) displays the temperature dependence of resistivity (ρ) for $EuFe_2P_2$. The room-temperature resistivity is ~ 0.15 mΩ cm, which is nearly the same to that of polycrystalline sample of $BaFe_2P_2$,[31] but about one order of magnitude smaller than the value of $EuFe_2As_2$.[10] Unlike $EuFe_2As_2$ which shows two anomalies in ρ at 20 and 200 K, there is only one resistivity anomaly in $EuFe_2P_2$, i.e., a kink at 29.2 K, corresponding to the aforementioned ferromagnetic transition in Eu sublattice. The residual resistivity ratio, defined as $\rho_{300\ K}/\rho_{2\ K}$, is ~ 40, much reduced in comparison with that of $BaFe_2P_2$(~ 70).[31] This result suggests additional magnetic scattering due to the Eu^{2+} moments in $EuFe_2P_2$. For *simplicity*, we roughly assume that the resistivity contribution from electron-phonon scattering, denoted by $\rho_{e\text{-}ph}(T)$, is the same for both materials. Then, the resistivity contribution from magnetic scattering [$\rho_{mag}(T)$] in $EuFe_2P_2$ can be obtained simply by a subtraction. As can be seen in Fig. 7(a), the $\rho_{mag}(T)$ data show a maximum at ~ 55 K, which is reminiscence of dense Kondo behavior in other systems such as

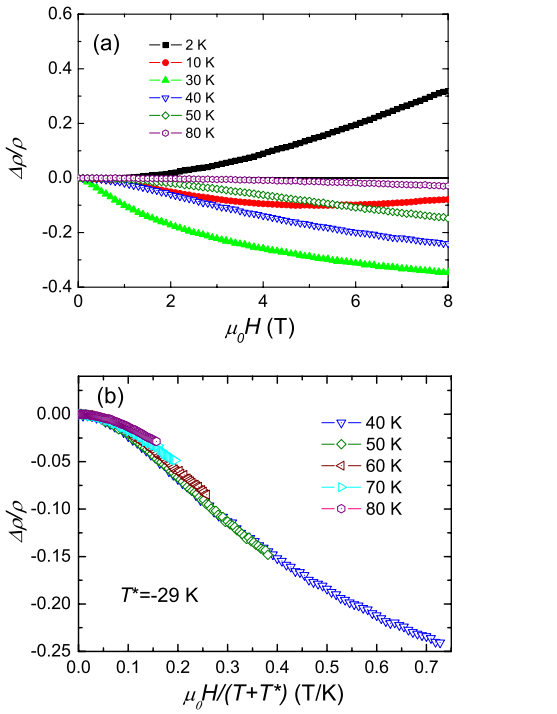

FIG. 8. (Color online) (a) Isothermal magnetoresistance for $EuFe_2P_2$ at different temperatures. (b) Scaling behavior of the magnetoresistance in $EuFe_2P_2$.

CeTSb$_2$ (Ref. 32) and $CeNiGe_3$ material.[33] It is noted that upon applying a pressure up to 4 GPa, a broad resistivity peak appears around 100 K without the subtraction of $\rho_{e\text{-}ph}(T)$.[34] This pressure-enhanced Kondo effect is very common[35] because the 4f level tends to approach Fermi energy with increasing pressure.

Under an 8 T field, there is negligible effect on $\rho(T)$ above 80 K. However, anomalous temperature-dependent MR is observed below 80 K, as illustrated clearly in Fig. 7(b). Namely, a negative MR grows with decreasing temperature below 80 K and reaches its minimum of -35% at the FM ordering temperature. Then the negative MR decreases with further decreasing temperature and finally undergoes sign reversal around 10 K, below which positive MR increases with decreasing temperature and achieves 35% at 2 K. It is noted that the resistivity kink at 29.2 K under zero field shifts to higher temperature (over 50 K) and becomes very much broadened by the external 8 T field. All the above MR behavior resembles those in $CeNiGe_3$,[33] except that the latter system has an AFM ground state.

The isothermal field dependence of MR for $EuFe_2P_2$ [Fig. 8(a)] gives further support for the dense Kondo behavior. For 40 K$\leq T \leq$80 K, the negative MR increases monotonically with increasing H and decreasing T, in agreement with a characteristic Kondo-type behavior. According to a theoretical result,[36] the magnetoresistance, $\Delta\rho/\rho_0$ can be scaled with $H/(T+T^*)$, where T^* is a measure of the single impurity Kondo energy scale. Figure 8(b) shows that the MR data between 40 and 80 K basically fall on the same curve for $T^*=-29$ K. The negative sign of T^*, with the absolute value close to the paramagnetic Curie temperature (θ) derived above, is consistent with the FM correlation in the system.

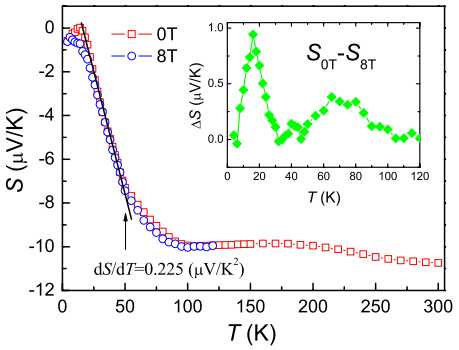

FIG. 9. (Color online) Temperature dependence of thermoelectric power for $EuFe_2P_2$. The inset shows the change in thermopower below the Curie temperature under an 8 T field.

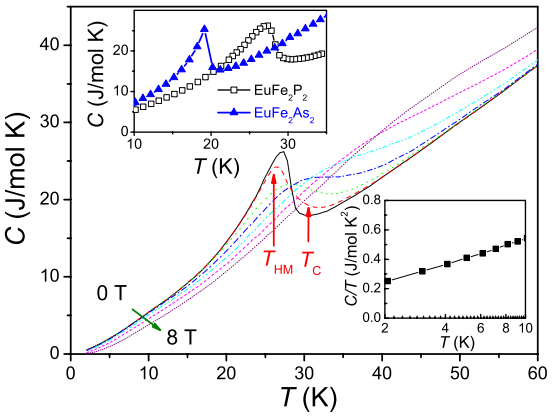

FIG. 10. (Color online) Temperature dependence of specific heat of $EuFe_2P_2$ under magnetic fields of 0, 0.2, 0.5, 1, 2, 4, and 8 T. The upper inset compares the $C(T)$ behavior with that of $EuFe_2As_2$. The lower inset plots C/T vs T for $EuFe_2P_2$.

This scaling behavior provides compelling evidence for the Kondo interaction in $EuFe_2P_2$.

2. Thermoelectric power

Figure 9 shows the temperature dependence of thermoelectric power or Seebeck coefficient (S) in $EuFe_2P_2$. The negative values of S in the whole temperature range indicate that electron transport is dominant. This is in contrast with the $S(T)$ behavior in $EuFe_2As_2$, which shows sign changes from negative to positive then to negative again with increasing temperature.[10] Above 100 K, the thermopower is about -10 μV/K, almost independent of temperature (note that the small gradual change from 200 to 300 K may due to the influence of trace amount of Fe_2P). Below 90 K, $|S|$ starts to decrease and it shows a linear behavior from 15 to 45 K. According to Behnia *et al.*,[37] the slope dS/dT correlates closely with the electronic specific-heat coefficient γ by a dimensionless quantity,

$$q = \frac{S}{T}\frac{N_A e}{\gamma}, \tag{2}$$

where $N_A e$ is the so-called Faraday number. For strongly correlated electron systems, the q value is close to unity.[37] Thus the electronic specific-heat coefficient in $EuFe_2P_2$ can be estimated to be ~ 220 mJ K^{-1} mol^{-1}, which is very close to the C/T value at 2 K (see below). This remarkably large value of γ is consistent with the Kondo behavior shown above.

Under a magnetic field of 8 T, the thermopower has a subtle change. By a simple subtraction, one can see a two-peak structure in the inset of Fig. 9. While the sharp peak at low temperatures is related to the FM state, the broad peak centered at 70 K should be associated with the dense Kondo effect, which is supposed to be suppressed by the external field. Further theoretical investigation is needed to clarify this phenomenon.

E. Specific heat

Figure 10 shows the specific-heat measurement result for $EuFe_2P_2$, especially in the lower temperature ranges. Under zero field, a specific-heat anomaly appears below 29 K, corresponding to the FM and HM transitions of Eu^{2+} sublattice. The HM transition at $T_{HM}=26$ K is inferred by comparing the $C(T)$ behavior with that of $EuFe_2As_2$, as shown in the upper inset of Fig. 10. While $EuFe_2As_2$ shows a sharp peak at 19 K, $EuFe_2P_2$ exhibits a round broader peak at 27 K, suggesting a superposition of two nearby transitions. The successive transition is further demonstrated by the decrease in T_{HM} and an increase in T_C with the applied field of 0.2 T. The released magnetic entropy up to the Curie temperature was estimated (the phonon background is assumed to obey Debye model) about 80% of R ln 8 (where R represents gas constant), implying the contribution from Kondo state at high temperatures.

Owing to the FM/HM transitions, it is difficult to extract the electronic specific-heat coefficient by a conventional method. Thus we simply consider C/T, shown in the lower inset of Fig. 10. Since the phonon and magnon contributions are estimated to be negligibly small at 2 K (since $\theta_D \gg 2$ K and $T_C \gg 2$ K), the real electronic specific-heat coefficient would be not so much smaller than $C/T|_{T=2\ \mathrm{K}} \approx 250$ mJ K^{-1} mol^{-1}. This result is consistent the above indirect estimation from the thermopower measurement.

Under magnetic fields, the specific-heat anomaly moves to higher temperatures, and the peak becomes more and more broadened with increasing fields. This result is consistent with the above magnetization measurement, suggesting dominant FM alignment and stronger FM correlations in $EuFe_2P_2$, in comparison with the A-type antiferromagnet $EuFe_2As_2$.[14,18,19]

F. Further discussion

Now let us discuss why the sister compounds $EuFe_2P_2$ and $EuFe_2As_2$ behave so differently. First, according to the argument by Si and Abrahams,[38] the loss of Fe moments is due to the relatively weak $3d$ electron correlation in iron *phosphides*. So far, there is no report on the appearance of Fe local moments in the iron phosphides with $ThCr_2Si_2$-type structure. Second, the difference in the magnetic order of Eu $4f$ moments has to be explained in terms of an indirect

RKKY interactions because the Eu-interlayer spacing is much larger than the expected spacing for a direct exchange. The RKKY exchange coupling $J_{RKKY} \propto -\frac{\alpha \cos \alpha - \sin \alpha}{\alpha^4}$, where $\alpha = 2k_F R$, R denotes the distance between two magnetic moments and k_F the Fermi wave vector. Upon changing $2k_F R$, J_{RKKY} alters greatly, or even changes the sign. In going from $EuFe_2As_2$ to $EuFe_2P_2$, R decreases from 6.06 to 5.64 Å. Even if k_F remains constant, the decrease in R may alter J_{RKKY} remarkably, which would result in a crossover from AFM to FM ordering. Note that the FM order of Eu^{2+} moments in $EuFe_{2-x}Ni_xAs_2$ system was explained as a result of the decrease in α.[30] In fact, the change in $J_{RKKY}(R, k_F)$ can be very minute, as manifested by the helimagnetism in $Eu(Fe_{0.89}Co_{0.11})_2As_2$.[28] It is in principle possible that successive magnetic transitions may occur when decreasing temperature.

The observed dense Kondo behavior in $EuFe_2P_2$ could be attributed to the proximity of the $4f$ level to Fermi energy.[5] To our knowledge, dense Kondo behavior in Eu-containing compounds is rarely discovered,[39] primarily because Eu^{2+} carries a large moment. Kondo effect involves the intrasite coupling between local moment and conduction carriers while the RKKY interaction is a long-range intersite magnetic exchange through conduction carriers. Therefore, the interplay between Kondo and RKKY interactions is inevitable. In the ground state of $EuFe_2P_2$, according to the well-known Doniach scenario,[40] the RKKY interaction prevails against the Kondo effect in $EuFe_2P_2$. Since applying pressure enhances the Kondo effect,[34] the isovalent chemical doping in $EuFe_2P_2$ should be promising to tune the ground state in this intriguing system.

IV. CONCLUDING REMARKS

In summary, we have performed a systematic research on a ternary iron phosphide $EuFe_2P_2$. This compound shows contrasting physical properties with its analog $EuFe_2As_2$, although both materials contains Eu^{2+} and without P-P covalent bonding. The result indicates dominant FM ordering for the Eu sublattice. However, the ground state has a possible helimagnetic ordering with the moments basically parallel to the c axis. Future neutron diffractions are expected to resolve this issue. On the other hand, the magnetotransport properties governed by the itinerant Fe $3d$ electrons show a dense Kondo behavior. Future measurements using single crystalline samples may confirm this point, and more information on the anisotropic property are also expected.

Moreover, alloys of $EuFe_2P_2$ and $EuFe_2As_2$ exhibits coexistence of high-temperature superconductivity and local-moment ferromagnetism.[12] Therefore, $EuFe_2P_2$ and its related materials deserve further exploration with regard to the interplay of Kondo, RKKY, and Cooper-pairing interactions among $4f$ and conduction electrons.

ACKNOWLEDGMENTS

This work is supported by the National Basic Research Program of China (Grant No. 2007CB925001), National Science Foundation of China (Grant No. 10934005), and the Fundamental Research Funds for the Central Universities of China (No. 2010QNA3026). The research in Jerusalem is partially supported by the Israel Science Foundation (ISF, Bikura Grant No. 459/09) and by the Klachky Foundation for Superconductivity.

*Corresponding author; ghcao@zju.edu.cn

[1] H. B. Radousky, *Magnetism in Heavy Fermion Systems* (World Scientific, Singapore, 2000).
[2] G. R. Stewart, Rev. Mod. Phys. **56**, 755 (1984).
[3] E. Mörsen, B. D. Mosel, W. Müller-Warmuth, M. Reehuis, and W. Jeitschko, J. Phys. Chem. Solids **49**, 785 (1988).
[4] C. Huhnt, W. Schlabitz, A. Wurth, A. Mewis, and M. Reehuis, Physica B **252**, 44 (1998).
[5] B. Ni, M. M. Abd-Elmeguid, H. Micklitz, J. P. Sanchez, P. Vulliet, and D. Johrendt, Phys. Rev. B **63**, 100102(R) (2001).
[6] E. R. Bauminger, D. Froindlich, I. Nowik, S. Ofer, I. Felner, and I. Mayer, Phys. Rev. Lett. **30**, 1053 (1973).
[7] C. U. Segre, M. Croft, J. A. Hodges, V. Murgai, L. C. Gupta, and R. D. Parks, Phys. Rev. Lett. **49**, 1947 (1982).
[8] R. Marchand and W. Jeitschko, J. Solid State Chem. **24**, 351 (1978).
[9] H. Raffius, E. Mörsen, B. D. Mosel, W. Müller-Warmuth, W. Jeitschko, L. Terbüchte, and T. Vomhof, J. Phys. Chem. Solids **54**, 135 (1993).
[10] Z. Ren, Z. W. Zhu, S. Jiang, X. F. Xu, Q. Tao, C. Wang, C. M. Feng, G. H. Cao, and Z. A. Xu, Phys. Rev. B **78**, 052501 (2008).
[11] M. Tegel, M. Rotter, V. Weib, F. M. Schappacher, R. Pottgen, and D. Johrendt, J. Phys.: Condens. Matter **20**, 452201 (2008).
[12] Z. Ren, Q. Tao, S. Jiang, C. M. Feng, C. Wang, J. H. Dai, G. H. Cao, and Z.-A. Xu, Phys. Rev. Lett. **102**, 137002 (2009).
[13] H. S. Jeevan, Z. Hossain, D. Kasinathan, H. Rosner, C. Geibel, and P. Gegenwart, Phys. Rev. B **78**, 092406 (2008).
[14] S. Jiang, Y. K. Luo, Z. Ren, Z. W. Zhu, C. Wang, X. F. Xu, Q. Tao, G. H. Cao, and Z.-A. Xu, New J. Phys. **11**, 025007 (2009).
[15] D. Wu, N. Barisic, N. Drichko, S. Kaiser, A. Faridian, M. Dressel, S. Jiang, Z. Ren, L. J. Li, G. H. Cao, Z. A. Xu, H. S. Jeevan, and P. Gegenwart, Phys. Rev. B **79**, 155103 (2009).
[16] C. F. Miclea, M. Nicklas, H. S. Jeevan, D. Kasinathan, Z. Hossain, H. Rosner, P. Gegenwart, C. Geibel, and F. Steglich, Phys. Rev. B **79**, 212509 (2009).
[17] T. Terashima, M. Kimata, H. Satsukawa, A. Harada, K. Hazama, S. Uji, H. S. Suzuki, T. Matsumoto, and K. Murada, J. Phys. Soc. Jpn. **78**, 083701 (2009).
[18] J. Herrero-Martín, V. Scagnoli, C. Mazzoli, Y. Su, R. Mittal, Y. Xiao, Th. Brueckel, N. Kumar, S. K. Dhar, A. Thamizhavel, and L. Paolasini, Phys. Rev. B **80**, 134411 (2009).
[19] Y. Xiao, Y. Su, M. Meven, R. Mittal, C. M. N. Kumar, T. Chatterji, S. Price, J. Persson, N. Kumar, S. K. Dhar, A. Thamizhavel, and Th. Brueckel, Phys. Rev. B **80**, 174424 (2009).
[20] G. F. Chen, Z. Li, D. Wu, G. Li, W. Z. Hu, J. Dong, P. Zheng, J. L. Luo, and N. L. Wang, Phys. Rev. Lett. **100**, 247002 (2008).
[21] E. M. Brüning, C. Krellner, M. Baenitz, A. Jesche, F. Steglich, and C. Geibel, Phys. Rev. Lett. **101**, 117206 (2008).

[22] F. Izumi, Mater. Sci. Forum **321-324**, 198 (2000).
[23] I. Nowik and I. Felner, Hyperfine Interact. **28**, 959 (1986).
[24] R. Hoffmann and C. Zheng, J. Phys. Chem. **89**, 4175 (1985).
[25] I. D. Brown and D. Altermatt, Acta Crystallogr., Sect. B: Struct. Sci. **41**, 244 (1985).
[26] N. E. Brese and M. OKeeffe, Acta Crystallogr., Sect. B: Struct. Sci. **47**, 192 (1991).
[27] S. Chiba, J. Phys. Soc. Jpn. **15**, 581 (1960).
[28] S. Jiang, H. Xing, G. F. Xuan, Z. Ren, C. Wang, Z. A. Xu, and G. H. Cao, Phys. Rev. B **80**, 184514 (2009).
[29] I. Nowik and I. Felner, Physica C **469**, 485 (2009).
[30] Z. Ren, X. Lin, Q. Tao, S. Jiang, Z. W. Zhu, C. Wang, G. H. Cao, and Z.-A. Xu, Phys. Rev. B **79**, 094426 (2009).
[31] S. Jiang, H. Xing, G. F. Xuan, C. Wang, Z. Ren, C. M. Feng, J. H. Dai, Z. A. Xu, and G. H. Cao, J. Phys.: Condens. Matter **21**, 382203 (2009).
[32] Y. Muro, N. Takeda, and M. Ishikawa, J. Alloys Compd. **257**, 23 (1997).
[33] A. P. Pikul, D. Kaczorowski, T. Plackowski, A. Czopnik, H. Michor, E. Bauer, G. Hilscher, P. Rogl, and Y Grin, Phys. Rev. B **67**, 224417 (2003).
[34] Y. Uwatoko *et al.* (private communications).
[35] J. D. Thompson and Z. Fisk, Phys. Rev. B **31**, 389 (1985).
[36] P. Schlottmann, Phys. Rep. **181**, 1 (1989).
[37] K. Behnia, D. Jaccard, and J. Flouquet, J. Phys.: Condens. Matter **16**, 5187 (2004).
[38] Q. Si and E. Abrahams, Phys. Rev. Lett. **101**, 076401 (2008).
[39] C. D. Cao, R. Klingeler, N. Leps, H. Vinzelberg, V. Kataev, F. Muranyi, N. Tristan, A. Teresiak, S. Q. Zhou, W. Loser, G. Behr, and B. Buchner, Phys. Rev. B **78**, 064409 (2008).
[40] S. Doniach, *Valence Instabilities and Related Narrow Band Phenomena*, edited by R. D. Parks (Plenum, New York, 1977).